J. Membrane Biol. 103, 171–180 (1988)

The Journal of
Membrane Biology

Ion Permeation and Rectification in ATP-Sensitive Channels from Insulin-Secreting Cells (RINm5F): Effects of K^+, Na^+ and Mg^{2+}

S. Ciani and B. Ribalet

Department of Physiology, Ahmanson Laboratory of Neurobiology, Brain Research Institute, and Jerry Lewis Neuromuscular Research Center, University of California, Los Angeles, California 90024

Summary. Patch-clamp techniques were used to study the permeability to ions of an ATP-sensitive channel in membranes from the pancreatic B-cell line (RINm5F). With patches in the outside-out configuration, the *I-V* curves for different Na^+-K^+ mixtures in the bath and 140 mM K^+ in the pipette were almost linear, and crossed the zero-current axis at voltages that indicated a variable permeability ratio. When K^+ was added symmetrically, the plot of the conductance *vs.* K^+ activity exhibited saturation, with a G_{max} of about 160 pS and a half-maximal activity of 216 mM. The *I-V* behavior for different K^+-Na^+ mixtures in the bath could be accurately described with a model based on Eyring theory, assuming two sites and one-ion occupancy. For K^+, the dissociation constants ($\bar{K}_K$) of the two sites were 290 and 850 mM, the lower value pertaining to the site close to the intracellular medium. In experiments with inside-out patches, both Na^+ and Mg^{2+}, when present in the bath, induced a voltage-dependent block of the outward current. Fitting the data with the model suggested that for these ions only one of the two sites binds significantly, the corresponding dissociation constants being (mM): 46 for Na^+ and 34 for Mg^{2+}. Blocking by Na^+ and Mg^{2+} may account for the low outward current seen in intact cells. This hypothesis is consistent with the observation that such current is further reduced by addition of 2,4-DNP, since metabolism inhibitors are expected to lower the ATP level, thereby liberating Mg^{2+} from the Mg^{2+}-ATP complex, as well as inducing accumulation of Na^+ by decreasing the rate of the Na^+-K^+ pump.

Key Words B-cell · ATP-dependent K channel · ion permeability · Na^+ and Mg^{2+} blocking · mitochondrial inhibitor

Introduction

Cell-attached patches of pancreatic B-cell membranes from adult rats, as well as from the insulinoma cell line RINm5F, have a K-selective pore that is closed by glucose (Ashcroft, Harrison & Ashcroft, 1984; Rosman & Trube, 1985; Misler et al., 1986; Ribalet & Ciani, 1987). This glucose-sensitive K channel was identified, in excised patches, with a channel that has similar conductive and kinetic properties and is blocked by addition of ATP to the intracellular medium (Cook & Hales, 1984; Findlay, Dunne & Petersen, 1985; Rorsman & Trube, 1985; Misler et al., 1986; Ribalet & Ciani, 1987). A similar ATP-sensitive channel has also been found in cardiac (Noma, 1983) and skeletal muscle (Spruce, Standen & Stanfield, 1985). Although its function in all these tissues is not understood completely, inhibition of channel activity in pancreatic B-cells by subthreshold levels of glucose is strongly suggestive of its being responsible for the initial depolarization and the decrease in potassium permeability observed in these cells with microelectrodes under similar conditions (Atwater, Ribalet & Rojas, 1978).

Using membrane patches from the RINm5F cell line, we have characterized some electrical properties of the ATP-sensitive channel in the presence of the physiologically relevant cations: K^+, Na^+, Mg^{2+}. Besides giving basic information about the biophysical characteristics of this channel, these studies will help answer the following questions: What causes the rectification, even when the channel is interposed between symmetrical K^+? Is this rectification similar to that of the "inward rectifier"? Is the channel capable of carrying significant outward current in physiological gradients of K^+, as would be expected if it regulates the membrane potential at rest?

Important permeability studies of the ATP-sensitive channel in heart, skeletal muscle, as well as in pancreatic B-cells have been reported already (Kakei, Noma & Shibasaki, 1985; Findlay, 1987; Horie, Irisawa & Noma, 1987; Spruce et al., 1987). The main objective of this paper is to provide a characterization of the *I-V* relationships in excised patches that is sufficiently detailed to allow a description of the data in terms of a simple model, as well as to use this model in the attempt to interpret observations of biological interest in intact cells.

Materials and Methods

Cell Culture

B-cells from the insulin-secreting cell line RINm5F, incubated in RPMI 1640 media supplemented with 10% fetal calf serum, 0.5% penicillin and 0.5% streptomycin, were kept in an atmosphere of 5% CO_2 and 95% air at a temperature of 37°C. The cells were divided once a week by treatment with trypsin, and the medium was changed twice between divisions.

Recording Methods

The single-channel conductance was studied with excised patches, both in the inside-out and in the outside-out configuration, as well as with on-cell patches. The method for preparing electrodes was similar to that described by Hamill et al. (1981). The pipettes were drawn using a vertical puller (Kopf Instruments), then coated with Sylgard® and fire polished. When filled with 140 mM KCl (or KAc), adequate electrodes would have a resistance in the order of 5 to 10 MΩ. According to standard methods, seals were formed by applying negative pressure. Once the seal formed on a cell, excised inside-out patches were obtained by withdrawing the pipette, while outside-out patches required, before pipette withdrawal, transition from the on-cell to the whole-cell configuration.

Single-channel currents, filtered at 1 or 2 kHz with a 6-pole Bessel filter, were recorded with an EPC 7 List amplifier. The data were stored on a videocassette recorder after digitalization using an audio processor (Bezanilla, 1985). To determine current–voltage relationships, steady voltages were applied to the patch pipettes for a few (5 to 10) sec. In the text and in the Figures, the sign of the potentials is that of the potential differences between the intracellular side of the patch and the extracellular one. Currents are considered positive when flowing in the outward direction.

Solutions

All the solutions were buffered to pH 7.2, using HEPES (10 mM). The ion composition in the bath solutions and in the electrodes will be specified in the Figure legends. Generally, the pipettes contained either 140 mM KCl or 135 mM KAc + 5 mM KCl. 2 mM $CaCl_2$ was also present in the pipette in experiments with excised inside-out patches. Potassium acetate was used in certain studies, due to the occasional appearance, in the presence of high concentration of Cl^- ions, of a large channel that was activated by hyperpolarizing the patch. When acetate was the main anion in the pipette, 5 mM KCl was also added in order to stabilize the potential between the metal electrode (Ag-AgCl) and the solution in the pipette. In the solutions bathing the intracellular side of the patch, no Ca^{2+} was added expressly, and 0.3 mM EGTA was used in some experiments. The reference electrode consisted of an agar solution of 140 mM KCl. Before forming the patch, the potential was adjusted to nullify the pipette current when the solutions in the pipette and in the bath had similar ionic composition (except for the 2 mM Ca^{2+}, which was present only externally). In this condition, the potential adjustment compensates for the sum of the two metal-liquid junction potentials and of the liquid-junction potential between the agar and the bath solution. The latter was calculated using the Henderson equation and assuming that the ionic diffusion coefficients in the gel are the same as in water. Once the patch was formed and the fluid in the bath eventually exchanged, the applied potentials (pipette potentials) were corrected for the difference between the junction potential calculated in the new condition and the initial one. The largest correction, corresponding to replacement of 140 mM KAc with 135 mM NaAc and 5 mM KCl, was about 4 mV. In these calculations, as well as in the equations of the model, activities were used instead of concentrations (except for Mg^{2+}). The single-ion activity coefficients were calculated from tabulated activity coefficients of the electrolytes, using the theory of Debye and Huckel. In mixtures of electrolytes, the mean activity coefficient was taken to be the weighted average of those of the individual electrolytes.

Data Analysis

For analysis, the single-channel current fluctuations were played back either on a strip-chart recorder, or, alternatively, were loaded onto an IBM computer via a double-memory buffer interface which allows transfer of data points in a continuous mode on a Winchester type drive. When the current steps had long opening times and uniform sizes, their average amplitudes were measured by hand from play-backs on the strip-chart recorder or an oscilloscope. Alternatively, they were calculated from computer-built amplitude histograms. Most of the data represented in each figure refer to series of experiments performed on the same patch. Error bars, indicating the variability of the current, were added when the measurement was repeated several times in the same conditions with different patches. However, all the experiments have been carried out more than once.

The theoretical fits were carried out by computer, using a standard "least-squares" minimization routine for nonlinear functions.

Results

Cell-Attached and Outside-Out Patches. Effects of K^+ and External Na^+

Openings of glucose-sensitive K channels are seen frequently in cell-attached patches of B-cell membranes. Figure 1 shows recordings of one such current, as well as the corresponding *I-V* relationship. Although the K^+ levels on both sides of the channel were presumably similar, since the pipette contained 140 mM KCl, the current was asymmetrical around the reversal potential: it was nearly linear with voltage when it flowed into the cell, but saturated in the outward direction. This type of behavior may arise from asymmetries in the energy profile of the ionic pathway, but may also be due to blocking by poorly permeant intracellular ions. According to recent reports, the latter hypothesis applies probably to the "inward rectifier" in cardiac cells, as well as to the ATP-channel both in cardiac and pancreatic B-cells, where blocking by intracellular Mg^{2+} appears to be the main cause for saturation of

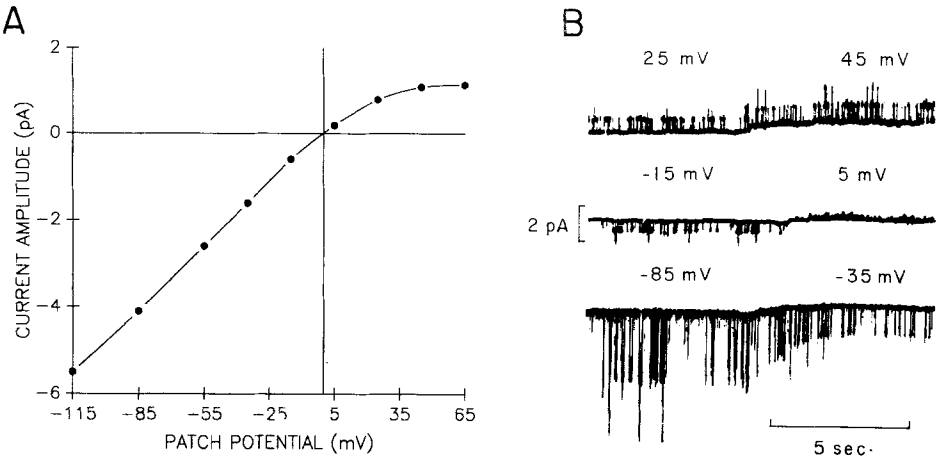

Fig. 1. (*A*) *I-V* relationship for the ATP-channel in a cell-attached patch with 140 mM KCl in the pipette. The bath solution contained (mM): 135 NaCl, 5 KCl, 2.5 $CaCl_2$, 1.1 $MgCl_2$, 5 HEPES (pH 7.2). The patch potential was estimated assuming an intracellular K^+ concentration of 140 mM and correcting for junction potentials as described in Materials and Methods. The line through the data points was drawn by hand. (*B*) Single-channel current steps, corresponding to the experiment in (*A*), at different patch potentials. Downward deflections indicate inward current. The traces were filtered at 1 kHz

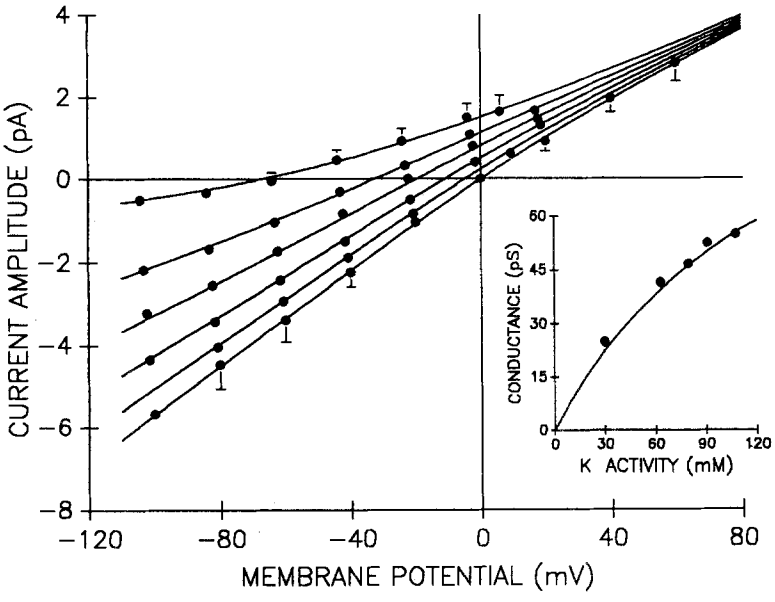

Fig. 2. *I-V* relationships for an ATP channel in an excised outside-out patch with different Na^+-K^+ mixtures in the bath; $[Na^+]$ + $[K^+]$ = 140 mM. Starting from the top, $[K^+]$ was (mM): 5, 33, 59, 86, 114, 140. Acetate instead of Cl^- was used for the reasons stated in Materials and Methods. $[CaCl_2]$, $[MgCl_2]$ and pH in the bath were as in Fig. 1. The electrode contained 140 mM K^+ (135 mM KAc + 5 mM KCl). The error bars give the maximum deviation from the average seen in nine experiments for $[K^+]$ = 140 mM and five for $[K^+]$ = 5 mM. The inset gives a plot of the conductance (estimated from the current at 40 mV away from equilibrium) against the K^+ activity for patches between symmetrical solutions. The continuous curves are fits to the data with a three-barrier model (*see* Fig. 6). The fitting parameters are described in the text and listed in the Table

the outward current (Findlay, 1987; Horie et al., 1987; Matsuda, Saigusa & Irisawa, 1987; Vanderberg, 1987). In order to study the properties of the ATP-sensitive channel in conditions of known ion composition, experiments were performed with excised patches. Figure 2 shows six *I-V* relationships, all obtained from one patch in the outside-out configuration. Each set of aligned points corresponds to a different mixture of K^+ and Na^+ in the bath (solution external to the cell), with the sum of the concentrations constant and equal to 140 mM. K^+ in the pipette was 140 mM (135 mM KAc + 5 mM KCl). When the bath contained 5 mM K^+ and 135 mM Na^+, the zero-current potential across the patch was about −65 mV. Different patches in similar conditions gave values in the range between −63 and −70 mV. Similar reversal potentials were obtained when sulfate or Cl^- were used instead of acetate, whereas more negative ones (−75 mV) were found when Na^+ was replaced by choline, suggesting that the deviations from Nernstian behavior for K^+ in Fig. 2 are probably due to a significant permeability of the channel to Na^+. Using the constant-field equation, the permeability ratio, P_{Na}/P_K,

was found to be about 0.025 at low external K^+, but increased as the reversal potential became less negative. Somewhat smaller values (0.015) have been found for similar channels in cardiac and skeletal muscle (Kakei et al., 1985; Spruce et al., 1987). Single-channel currents were also measured in conditions in which the K^+ concentration was increased symmetrically on both sides of the membrane. As shown in the inset to Fig. 2, where each point corresponds to a different patch (since the solution had to be changed also in the pipette), the conductance increased with the activity of potassium, bending toward saturation. In these experiments, the conductance was estimated applying 40 mV to the patch in either direction. All the data in Fig. 2 could be accounted for by a one-ion, three-barrier model based on Erying rate reaction theory, even by using the simplifying assumption that the peaks and the wells of the free energy profile are spaced uniformly (*see* Fig. 6). This simplification has been used for all monovalent cations, but not for Mg^{2+}. A similar model has also been proposed by Spruce et al. (1987) for the ATP-sensitive channel in skeletal muscle. The fit to our data, using Eq. (A5), is shown by the continuous lines in Fig. 2. Four independent parameters were determined for K^+: the dissociation constants of the two sites, 850 and 290 mM, and the two rate constants for moving out of the channel, 4.6×10^7 sec^{-1} and 3.3×10^8 sec^{-1}. (The corresponding values for the two latter constants in the Table are divided by the Avogadro number.) The site that binds K^+ more strongly ($\bar{K}_K$ = 290 mM) is the one close to the internal solution, and the lower rate constant is that for moving out of that site into the internal solution. Consistent with these data, the G_{max} and the half-maximal K^+ activity in the conductance-*vs.*-activity plot (inset to Fig. 2) are 160 pS and 216 mM, respectively. The fit also demanded that the peak of the central barrier, as seen from the two sites, be much lower than those of the lateral barriers (*see* Fig. 6). Consequently, moving across the middle barrier is not rate limiting, implying that the rate constants for that step cannot be accurately determined. In this respect, our model is closer to that for the K^+ channel of the sarcoplasmic reticulum (Coronado, Rosenberg & Miller, 1980) than to the model for the ATP-sensitive channel in muscle proposed by Spruce et al. (1987).

Effects of Internal Na^+ and Mg^{2+}

Excised inside-out patches have been used to test the effects of Na^+ and Mg^{2+} in the solutions bathing the intracellular side of the channel. With 140 mM potassium on both sides of the patch, and in the absence of either Na^+ or Mg^{2+}, the *I-V* relationship

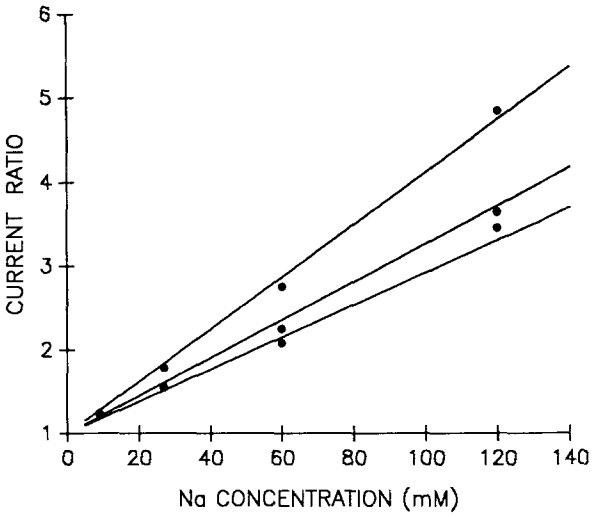

Fig. 3. Effects of internal Na^+. For excised inside-out patches with 140 mM K^+ in the pipette and 140 mM K^+ + *x* mM Na^+ in the bath, the ratios of the single-channel currents in the absence of Na^+ to those in the presence of Na^+ are plotted as a function of the *x* mM Na^+ in the bath. The three sets of points, all obtained with the same patch, correspond to three different membrane potentials (mV): (starting from the bottom), 30, 40, 60. The fit indicated a binding site with $\bar{K}_{Na}$ = 46 mM

was similar to that shown by the curve at the bottom in Fig. 2, which was obtained from an experiment with an outside-out patch. The weak rectification exhibited in this case (in conditions of symmetrical K^+ and with no other permeant ion present) is consistent with the values of the parameters estimated from the data in Fig. 2, and can be expected intuitively if one considers the asymmetry in the energy profile that they imply. However, when Na^+ was added to the bath (intracellular medium in this configuration of the patch), the outward current decreased, the strength of the effect depending both on the Na^+ level and the membrane voltage. The three sets of aligned points in Fig. 3, corresponding to three different membrane potentials, are ratios of currents in pure K^+ to those in mixtures with Na^+ in the bath, as a function of the Na^+ concentration in the bath. The data, all obtained from one patch, show that both depolarization of the patch and increase of internal Na^+ enhance the block of the outward current. The continuous curves represent a fit to the data with the following expression, obtained from Eq. (A6) in the Appendix:

$$\frac{I}{I(\mathrm{Na})} = 1 + \frac{(e^{2\phi/3}/\bar{K}^{e}_{Na}) + (e^{\phi/3}/\bar{K}^{i}_{Na})}{1 + e^{\phi/3}Q_K/M_K} a''_{Na}. \qquad (1)$$

α_{Na} is the activity of sodium, $\bar{K}^{e}_{Na}$ is the dissociation constant of the Na^+-binding site close to the external solution and $\bar{K}^{i}_{Na}$ that of the site close to the

Table. Fitting values of rate and equilibrium constants for permanent and blocking ions in the ATP channel of RINm5F cells[a]

	K^+	Na^+	Mg^{2+}
$\bar{\nu}'$(liter/sec) × 10^{16}	6.57	0.162	—
$\bar{\nu}''$(liter/sec) × 10^{16}	2.67	$\gg\bar{\nu}'$	—
$\bar{\mu}'$(mole/sec) × 10^{16}	0.77	—	—
$\bar{\mu}''$(mole/sec) × 10^{16}	5.59	(0.92)	—
$\bar{K}''(M) = \bar{\mu}''/\bar{\nu}'$	0.850	(5.660)	—
$\bar{K}'(M) = \bar{\mu}'/\bar{\nu}''$	0.290	0.046	0.034

[a] All the constants for K^+ (1st column), as well as the rate constant for Na^+, $\bar{\nu}^i_{Na}$, were calculated by fitting the data in Fig. 2 with Eq. (A5). The remaining parameters, deduced from experiments with mixtures of K^+ and the other ions, were estimated retaining the same values of the constants for K^+. Although no formal mathematical method has been used to estimate the errors for the parameters, the fit became visibly worse when variations by 20% or more were imposed on the values listed above, except for those within parentheses. The latter, which refer to the weakly binding site for Na^+, are certainly affected by large errors, since varying their values by even more than 100% had little effect on the fit.

internal one. The quantities M_K and Q_K are defined in the Appendix [*see* Eq. (A2)] and contain parameters pertaining only to K^+. Using the values deduced from the data of Fig. 2 for these parameters, the fit to the experiments in Fig. 3 gave very different numbers for $\bar{K}^e_{Na}$ and $\bar{K}^i_{Na}$ (*see* Table). Only the site close to the internal medium was found to bind significantly: $\bar{K}^i_{Na}$ = 46 mM. Note that this value denotes a binding strength for sodium almost one order of magnitude higher than for potassium.

Figure 4 illustrates the block of the current by internal Mg^{2+} with 140 mM K^+ on both sides of the patch. The current ratio (ratio of the current in the absence of Mg^{2+} to that in the presence of it) is plotted here as a function of voltage, with the four sets of points referring to different concentrations of Mg^{2+} in the bath (intracellular solution). All the points shown in the Figure were calculated from *I-V* curves obtained with one patch. Qualitatively, the effect on the K current is similar to that of Na^+, although the dependence on membrane potential is stronger. For Mg^{2+} concentrations of 5 mM and higher, the *I-V* relationship showed clear maxima for the outward current, although the zero-current potential remained unchanged, indicating that the channel is virtually impermeable to this ion. Assuming that the energy profile for Mg^{2+} in the channel can be schematized by one site only, accessible from the interior but separated from the exterior by an infinitely high barrier, the current ratio is found to be

$$\frac{I}{I(\mathrm{Mg})} = 1 + \frac{e^{2\alpha\phi}/\bar{K}_{Mg}}{1 + e^{\phi/3}Q_K/M_K}\, c^{\prime\prime}_{Mg} \qquad (2)$$

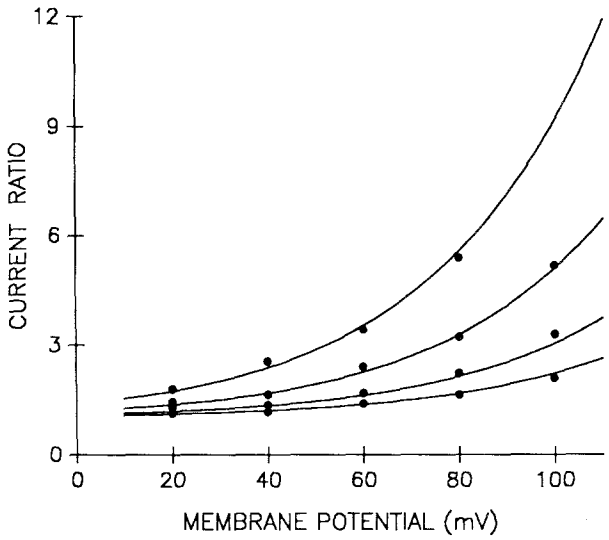

Fig. 4. Effects of internal Mg^{2+}. For excised inside-out patches with 140 mM K^+ in the pipette and 140 mM K^+ + *x* mM Mg^{2+} in the bath ($MgSO_4$), the ratio of the single-channel current in the absence of Mg^{2+} to that in the presence of Mg^{2+} in the bath is plotted against membrane voltage. Starting from the bottom, the four sets of points correspond to the following concentrations (mM) of Mg^{2+}: 2.2, 5, 10, 20. Modeling the channel as a one-site pore for Mg^{2+}, the fit to the data with Eq. (2) gave 34 mM for $\bar{K}_{Mg}$ and 0.35 for the "electrical" distance of the site from the internal solution

where $\bar{K}_{Mg}$ is the dissociation constant for Mg^{2+} and α is the "electrical" distance of the free-energy minimum from the inner mouth of the channel. The fit to the data (continuous curves in Fig. 4) gave for these quantities: 34 mM and 0.35, respectively. As in Eq. (1), the values of the rate constants for K^+ substituted in Eq. (2) were those deduced from the data in Fig. 2.

The experiments in Figs. 3 and 4 show that Na^+ and Mg^{2+}, when present in the solution bathing the cytoplasmic side of the membrane in an excised patch, have a blocking effect on the outward current. Considering that for concentrations similar to those existing intracellularly both ions block the outward current in experiments with excised patches, it seems reasonable to propose that the same mechanism may account for the rectification in intact cells. Figure 5 shows two *I-V* relationships obtained with cell-attached patches: one in normal physiological conditions and the other in the presence of the metabolism inhibitor, 2,4-DNP (10^{-5} M). In the latter case, the outward current was reduced considerably. As will be discussed later, this effect is consistent with the hypothesis suggested above, since a depressed metabolism with low ATP production is likely to raise the intracellular concentrations of both Mg^{2+} and Na^+. Using the parameters deduced from the studies with excised patches, it

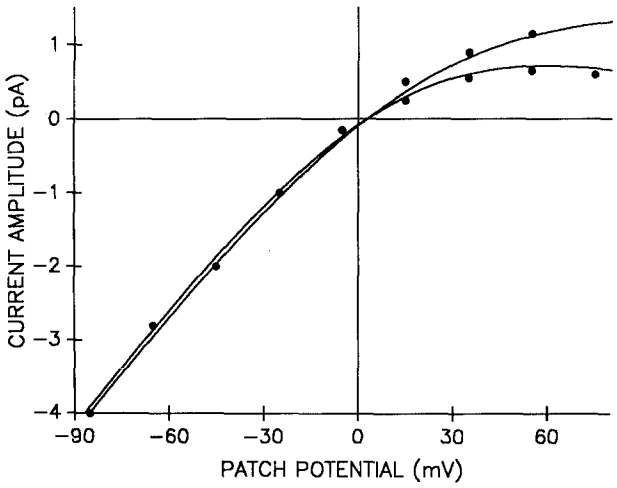

Fig. 5. Effect of the metabolic inhibitor 2,4-DNP. *I-V* relationship for a cell-attached patch in normal conditions (upper curve) and in the presence of 10^{-5} M DNP (lower curve). The ionic composition was as in Fig. 1. Using the parameters deduced from the data in Figs. 2, 3 and 4, an equation that combined the blocking effects of Na^+ and Mg^{2+} was used to fit the data by searching for the optimal values of the internal concentrations of K^+, Na^+ and Mg^{2+}. In the absence of DNP the values found were (mM): 120, 30 and 0.85; in the presence of it: 120, 33 and 9. The continuous curves are theoretical fits

will be actually argued that the transition from one *I-V* curve to the other in Fig. 5 is consistent with the order of magnitude of the changes in the levels of Na^+ and Mg^{2+} that can be expected from inhibition of the metabolism.

Discussion

Permeation and Block by Monovalent Cations: K^+ and Na^+

Using single-channel recording techniques in pancreatic B-cells from the RINm5F line, we have shown, both in this and in a previous paper (Ribalet & Ciani, 1987), that a metabolically regulated K channel which is seen in intact cells can also be found in isolated patches. Similar observations have been reported for B-cells obtained from primary cultures (for an extensive review of the literature *see* Petersen & Findlay, 1987). In Fig. 1, which refers to measurements on a cell-attached patch with 140 mM K^+ in the electrode, the K^+ concentrations on both sides of the channel were presumably similar. In this case, the current-voltage relationship should be comparable to the one that crosses the origin in Fig. 2 (excised outside-out patch). Although the outward current is lower in the cell-attached configuration, possibly due to blocking by intracellular ions, the inward currents in cell-attached and excised patches have very similar characteristics. This finding is important, inasmuch as it strongly suggests the identity of these channels and gives confidence in the significance of studying ionic permeabilities in conditions in which the composition of the solutions can be controlled on both sides of the membrane.

The zero-current potentials for the *I-V* curves in Fig. 2, all of which were obtained using the same outside-out patch with different K^+-Na^+ mixtures in the bath, indicate that the channel is considerably less permeable to Na^+ than to K^+; a result which basically agrees with previous data obtained in B-cells from neonatal rats (Cook & Hales, 1984), in cardiac cells (Kakei et al., 1985), as well as in skeletal muscle (Spruce et al., 1987). However, the permeability ratio, P_{Na}/P_K, as deduced from the zero-current potential applying the G-H-K equation, varies with the ionic conditions; more precisely, it increases as the reversal potential becomes less negative. Permeability ratios that depend on voltage are generally predicted by models for permeation based on Erying theory, as is the one in this paper, while constant values are expected only under special conditions (Läuger, 1973; Hille, 1975; Ciani, 1976). In our model, which assumes a low central energy barrier, the voltage-dependence of the permeability ratio is due to the fact that, for K^+, the ratio of the rate constants for entering the channel from the two sides, $\bar{\nu}'_K/\bar{\nu}''_K$, is very different from the corresponding ratio for Na^+. All the *I-V* curves in Fig. 2 are described using four independent parameters for K^+ (two rate constants for entering the channel, $\bar{\nu}'_K$, $\bar{\nu}''_K$ and two for getting out of it, $\bar{\mu}'_K$, $\bar{\mu}''_K$) and only one for Na^+, $\bar{\nu}'_{Na}$ (the rate constant for entering the channel from the external solution). The reason why only this constant was used for Na^+ in order to fit the data in Fig. 2 [neglecting the terms proportional to the Na^+ activity in the denominator of the general expression for the current, Eq. (A3)] can be justified in terms of the following circumstances: (a) the assumption, suggested by the strong asymmetry of the blocking effect, that Na^+ enters the channel much more easily from the intracellular solution than from the external one, namely $\bar{\nu}'_{Na}/\bar{\nu}''_{Na} \ll 1$; (b) the fact that in the experiments of Fig. 2 Na^+ was present only in the external solution. However, as it can easily be shown by an analysis of the equations of the model, a similar approximation is not valid when Na^+ is present inside. In this case, the term proportional to the activity of internal Na^+ in the denominator of Eq. (A3) must be considered. The fit to the results in Fig. 3 with Eq. (1) [which is deduced from Eq. (A6)] requires that

the site that binds Na^+ most strongly ($\bar{K}_{Na}$ = 46 mM) be the one closest to the internal solution. The dissociation constant of the other site is found to be much larger (5.6 M), but is a poorly defined parameter since large variations of its values have little effect on the fit. A model with only one site for Na^+ would have fitted the data in Fig. 3 equally well. However, for consistency it was preferred to use a model with two sites for monovalent cations, since two sites instead of one only give a much better description of the *I-V* curves for K^+ in the unblocked channel (e.g. in Fig. 2).

Effects of Internal Magnesium

Mg^{2+}, when present in the intracellular medium, blocks the single-channel K^+ current in a voltage-dependent manner without, however, altering the zero-current potential. Similar effects have been very recently reported for ATP-sensitive channels in cardiac cells (Horie et al., 1987) as well as in B-cells (Findlay, 1987). A quantitative description of the results was carried out, adopting a simple model whereby the block of the current would be due to binding of Mg^{2+} by a site located in the ionic pathway. The fit to the data with Eq. (2) gave a dissociation constant of about 34 mM and an "electrical distance" of 0.35, thus suggesting the presence of a site at about one-third of the channel length away from the inner mouth; virtually the same position as that of the strongly binding site for both Na^+ and K^+. The binding strength is somehow larger than for Na^+, and one order of magnitude greater than for K^+. The stronger voltage-dependence of blocking by Mg^{2+} as compared to Na^+ is plausibly due to its higher charge. It should be noted, however, that the effect of Mg^{2+} on this channel is weaker than in the case of the inward rectifier in cardiac cells, where submillimolar concentrations are sufficient to suppress the outward current (Matsuda et al., 1987; Vanderberg, 1987).

Effects of the Metabolism Inhibitor, 2,4-DNP and of Ouabain in Cell-Attached Patches

Figure 5 shows that addition of DNP (10^{-5} M) decreases significantly the outward current in cell-attached patches. Using the values for the various constants as determined from experiments with excised patches (*see* the Table), and searching for the concentrations of Na^+ and Mg^{2+} that optimized the fit to the data, the values calculated by computer were: (mM) 30 and 0.9 in the absence of the inhibitor, 33.5 and 9 in the presence of it. The theoretical fits for these values are shown by the continuous curves in Fig. 5. Although the ion composition of the RINm5F cells was not measured independently, the estimated levels for both Mg^{2+} and Na^+ in physiological conditions (absence of the inhibitor) are in good agreement with values determined previously for cells from various different tissues (Veloso et al., 1973; Saith, Bicknell & Schofield, 1984; Ng, Evans & Burke, 1987). From the values of the dissociation constants for Na^+ and Mg^{2+} (46.2 and 34 mM), one can see that in physiologically normal conditions, with an intracellular Mg^{2+} concentration close to 1 mM, most of the blocking of the outward current is due to Na^+. By contrast, the enhancement of such block upon addition of the inhibitor is interpreted (by the computer-based fitting routine) as being mainly due to increase in Mg^{2+}. The hypothesis that the Mg^{2+} level increases when metabolism inhibitors are added is supported by direct measurements with Mg^{2+}-sensitive dyes (Scarpa, 1974; DiPolo et al., 1976). Also the estimated value (9 mM) in the presence of DNP is not unreasonably high if one considers that: (a) the increase in free Mg^{2+} may primarily originate from dissociation of the Mg^{2+}-ATP complex, and (b) that comparably high ATP concentrations (9 mM) have been reported in pancreatic B-cells (Ashcroft, Ashcroft & Harrison, 1985). Given the strong binding constant of the Mg^{2+}-ATP complex (11,500 M^{-1}), as well as the fact that in the presence of metabolic inhibitors the total ATP level is known to drop by 80% of its original value (Ashcroft, Weerasinghe & Randall, 1973; Malaisse et al., 1979), high levels of Mg^{2+} in these conditions are to be expected. However, even if one accepts the 9 mM estimate of Ashcroft et al. (1985) for the intracellular concentration of ATP, Mg^{2+} buffers other than ATP, such as ADP or proteins from the endoplasmic reticulum and the Golgi complex (Clemente & Meldolesi, 1975; Phillips & Allison, 1977) will presumably bind some of the Mg^{2+} released by ATP, resulting in a concentration of free Mg^{2+} somewhat lower than 9 mM. A lower level of Mg^{2+} would not necessarily invalidate our model, since a good description of the data could still be obtained by moderately raising the level of Na^+. For example, a fit hardly distinguishable from that shown in Fig. 5 was found when Mg^{2+} was lowered from 9 to 6 mM and Na^+ raised from 33 to 41 mM. The latter value, which corresponds to a substantial increase in the level of Na^+, would be actually more consistent with the expectations, since the drop of ATP caused by DNP should inhibit the Na-K pump (Caldwell, 1960) and cause accumulation of Na^+. However, some uncertainty in the choice of the optimal values for the concentrations of Na^+ and Mg^{2+} is under-

standable, if one observes: (a) that the quantities that determine the efficacy of the block are the ratios of the ion concentrations to their respective dissociation constants, each multiplied by an exponential (larger for Mg^{2+} than for Na^+ when the potential is positive); and (b), that these quantities have similar values for the two ions in the range of the concentrations and potentials considered.

In view of these difficulties with the interpretation of experiments where the concentrations of Na^+ and Mg^{2+} vary simultaneously, it seemed interesting to test the effects of ouabain. Ouabain is known to specifically inhibit the Na-K pump without varying the level of ATP, and it is thus reasonable to expect that it will induce a change in Na^+ without substantially altering the level of Mg^{2+} (Baker, 1976). Addition of 10^{-4} M ouabain caused, within 15 to 20 min, a clear reduction of the outward current, although the effect was less pronounced than with DNP. Fixing the concentration of Mg^{2+} to 0.9 mM (the value deduced from the data in Fig. 5 in the absence of DNP), the fit to the current in the presence of ouabain estimated a Na^+ concentration of 41 mM; namely an increase of 11 mM with respect to the normal level. Although the danger of serious oversimplifications is present in this type of consideration based on indirect evidence, the value obtained is within plausible limits, since it is known that in different tissues similar concentrations of ouabain induce accumulation of Na^+ up to levels much higher than normal (Aikin, 1987). Even though the biological role of this block of the ATP channel by Na^+ and Mg^{2+} is not clear, it is tempting to speculate that it may serve as a safeguard mechanism to prevent rapid depletion of K^+ from cells with depressed metabolism.

We deeply thank Dr. M. Delay for guidance in the use of the data-fitting program. This research was supported by a grant from the National Science Foundation (DCB-85 17413), an award from the American Diabetes Association (W-P860812) and by a grant from the Muscular Dystrophy Association.

References

Aickin, C.C. 1987. Investigation of factors affecting the intracellular sodium activity in the smooth muscle of guinea-pig ureter. *J. Physiol. (London)* **385:**483–505

Ashcroft, F., Ashcroft, S., Harrison, D. 1985. The glucose-sensitive potassium channel in rat pancreatic beta-cells is inhibited by intracellular ATP. *J. Physiol. (London)* **369:**101P *(abstr.)*

Ashcroft, F.M., Harrison, D.E., Ashcroft, S.J.H. 1984. Glucose induces closure of single potassium channels in isolated rat pancreatic B-cells. *Nature (London)* **312:**446–448

Ashcroft, S.J.H., Weerasinghe, L.C.C., Randall, P.J. 1973. Interrelationship of islet metabolism, adenosine triphosphate content and insulin release. *Biochem. J.* **132:**223–231

Atwater, I., Ribalet, B., Rojas, E. 1978. Cyclic changes in potential and resistance of the B-cell membrane induced by glucose in islets of Langerhans from mouse. *J. Physiol. (London)* **278:**117–139

Baker, P.F. 1976. Regulation of intracellular Ca and Mg in squid axons. *Fed. Proc.* **35:**2589–2595

Bezanilla, F. 1985. A high capacity data recording device based on a digital audio processor and a video cassette recorder. *Biophys. J.* **47:**437–441

Caldwell, P.C. 1960. The phosphorus metabolism of squid axons and its relationship to the active transport of sodium. *J. Physiol. (London)* **152:**545–560

Ciani, S. 1976. Influence of molecular variations of ionophore and lipid on the selective ion permeability of membranes: II. A theoretical model. *J. Membrane Biol.* **30:**45–63

Clemente, F., Meldolesi, J. 1975. Calcium and pancreatic secretion. I. Subcellular distribution of calcium and magnesium in the exocrine pancreas of the guinea pig. *J. Cell Biol.* **65:**88–102

Cook, D.L., Hales, C.N. 1984. Intracellular ATP directly blocks K^+ channels in pancreatic B-cells. *Nature (London)* **311:**271–273

Coronado, R., Rosenberg, R., Miller, C. 1980. Ions selectivity, saturation, and block in a K^+-selective channel from sarcoplasmic reticulum. *J. Gen. Physiol.* **76:**425–446

Dipolo, R., Requena, J., Brinley, F.J., Mullins, L.J., Scarpa, A., Tiffert, T. 1976. Ionized calcium concentrations in squid axons. *J. Gen. Physiol.* **67:**433–467

Findlay, I. 1987. The effects of magnesium upon adenosine triphosphate-sensitive potassium channel in a rat insulin-secreting cell line. *J. Physiol. (London)* **391:**611–629

Findlay, I., Dunne, M.J., Petersen, O.H. 1985. ATP-sensitive inward rectifier and voltage- and calcium-activated K^+ channels in cultured pancreatic islet cells. *J. Membrane Biol.* **88:**165–172

Hamill, O.P., Marty, A., Neher, E., Sakmann, B., Sigworth, F.J. 1981. Improved patch-clamp techniques for high-resolution current recording from cells and cell-free membrane patches. *Pfluegers Arch.* **391:**85–100

Hille, B. 1975. Ionic selectivity, saturation, and block in sodium channels. A four-barrier model. *J. Gen. Physiol.* **66:**535–560

Horie, M., Irisawa, H., Noma, A. 1987. Voltage-dependent magnesium block of adenosine-triphosphate-sensitive potassium channel in guinea-pig ventricular cells. *J. Physiol. (London)* **387:**251–272

Kakei, M., Noma, A., Shibasaki, T. 1985. Properties of adenosine-triphosphate-regulated potassium channels in guinea-pig ventricular cells. *J. Physiol. (London)* **363:**441–462

Läuger, P. 1973. Ion transport through pores: A rate-theory analysis. *Biochim. Biophys. Acta* **311:**423–441

Malaisse, W.J., Hutton, J.C., Kawazu, S., Herchuelz, A., Valverde, I., Sener, A. 1979. The stimulus-secretion coupling of glucose-induced insulin release. XXXV. The links between metabolic and cationic events. *Diabetologia* **16:**331–341

Matsuda, H., Saigusa, A., Irisawa, H. 1987. Ohmic conductance through the inward rectifying K channel and blocking by internal Mg^{2+}. *Nature (London)* **325:**156–159

Misler, S., Falke, L.C., Gillis, K., McDaniel, M.L. 1986. A metabolite-regulated potassium channel in rat pancreatic B-cells. *Proc. Natl. Acad. Sci. USA* **83:**7119–7123

Ng, L.L., Evans, D.J., Burke, C.W. 1987. The human leucocyte sodium pump in adrenocortical insufficiency. *Clin. Endocrinol.* **72:**235–243

Noma, A. 1983. ATP-regulated K^+ channels in cardiac muscle. *Nature (London)* **305:**147–148

Petersen, O.H., Findlay, I. 1987. Electrophysiology of the pancreas. *Physiol. Rev.* **67:**1054–1116

Phillips, J.H., Allison, Y.P. 1977. The distribution of calcium, magnesium, copper and iron in the bovine adrenal medulla. *Neuroscience* **2:**147–152

Ribalet, B., Ciani, S. 1987. Regulation by cell metabolism and adenosine nucleotides of a K channel in insulin-secreting B-cells (RINm5F). *Proc. Natl. Acad. Sci. USA* **84:**1721–1725

Rorsman, P., Trube, G. 1985. Glucose dependent K^- channels in pancreatic B-cells are regulated by intracellular ATP. *Pfluegers Arch.* **405:**305–309

Scarpa, A. 1974. Indicators of free magnesium in biological systems. *Biochemistry* **13(14):**2789–2794

Saith, S., Bicknell, R.J., Schofield, J.G. 1984. Different sodium requirements for ^{86}Rb efflux and for growth hormone and prolactine secretion from bovine anterior pituitary cells. *Mol. Cell. Endocrinol.* **35:**47–54

Spruce, A., Standen, N., Stanfield, P. 1987. Studies of the unitary properties of adenosine-5′-triphosphate-regulated potassium channels of frog skeletal muscle. *J. Physiol. (London)* **382:**213–236

Spruce, A.E., Standen, N.B., Stanfield, P.R. 1985. Voltage-dependent ATP-sensitive potassium channels of skeletal muscle membrane. *Nature (London)* **316:**736–738

Vanderberg, C.A. 1987. Inward rectification of a potassium channel in cardiac ventricular cells depends on internal magnesium ions. *Proc. Natl. Acad. Sci. USA* **84:**2560–2564

Veloso, D., Guynn, R.W., Oskarsson, M., Veech, R.L. 1973. The concentrations of free and bound magnesium in rat tissues. *J. Biol. Chem.* **248:**4811–4819

Received 17 December 1987; revised 16 February 1988

Appendix

A Model Based on Eyring Theory for the ATP-Sensitive Pore. Single-Ion Occupancy

A) Two Species of Permeant Univalent Cations: K^+ and Na^+

A three-barrier model, similar to that drawn in Fig. 6, has been used to describe the ion fluxes across the ATP-sensitive channel in B-cells. The rate constants are denoted by ν', λ' and μ' for movement in the inward direction and by ν'', λ'' and μ'' for that in the outward one. When applied to activities or concentrations, the superscripts ′ and ″ refer to those on the extracellular and the intracellular side of the membrane, respectively. According to the formalism of the theory, the rate constants are exponential functions of the voltage. For example,

$$\nu' = \bar{\nu}' e^{-\beta\phi} \tag{A1}$$

where $\bar{\nu}'$ is independent of voltage, ϕ is the potential difference (in units of RT/F) across the whole channel, and β is the "electrical" distance between the site where the ion is located [the external mouth of the channel in the case of Eq. (A1)] and the top of the barrier it must cross. On account of the approximate linearity of the *I-V* curves when the channel is interposed between similar K^+ concentrations and when no blocking ion is present, the two following assumptions seemed justifiable, and were thus made in order to reduce the number of free parameters:

1) The energy wells (sites) are spaced uniformly, and the peaks are in the middle between consecutive sites. Thus, the "electrical" distance in the rate constants are all equal to $\frac{1}{6}$.

2) The peak of the central barrier, as viewed from either of the two internal sites, is much lower than those for leaving the channel. In terms of rate constants, $\bar{\mu} \ll \bar{\lambda}$. The second assumption is actually required to fit the data for the K^+ current in the absence of blocking, but has been postulated to hold true for Na^+ as well. Defining for brevity

$$M_i = \left(1 + \frac{\bar{\nu}_i'}{\bar{\nu}_i''} e^{2\phi/3}\right); \; N_i = \left(1 + \frac{\bar{\lambda}_i''}{\bar{\lambda}_i'} e^{\phi/3}\right);$$
$$Q_i = N_i \left(\frac{\bar{\nu}_i'}{\bar{\mu}_i'} a_i' e^{-\phi/3} + \frac{\bar{\nu}_i''}{\bar{\mu}_i'} a_i''\right) \; (i = K^+ \text{ or } Na^+) \tag{A2}$$

and using microscopic reversibility ($\bar{\nu}'\bar{\lambda}'\bar{\mu}' = \bar{\nu}''\bar{\lambda}''\bar{\mu}''$), the single-channel current carried by K^+ and Na^+ can be expressed in the form

$$I = -F \frac{\nu_K'(a_K' e^{-\phi/2} - a_K'' e^{\phi/2}) + \frac{M_K}{M_{Na}} \bar{\nu}_{Na}'(a_{Na}' e^{-\phi/2} - a_{Na}'' e^{\phi/2})}{M_K e^{-\phi/3} + Q_K + \frac{M_K}{M_{Na}} Q_{Na}}. \tag{A3}$$

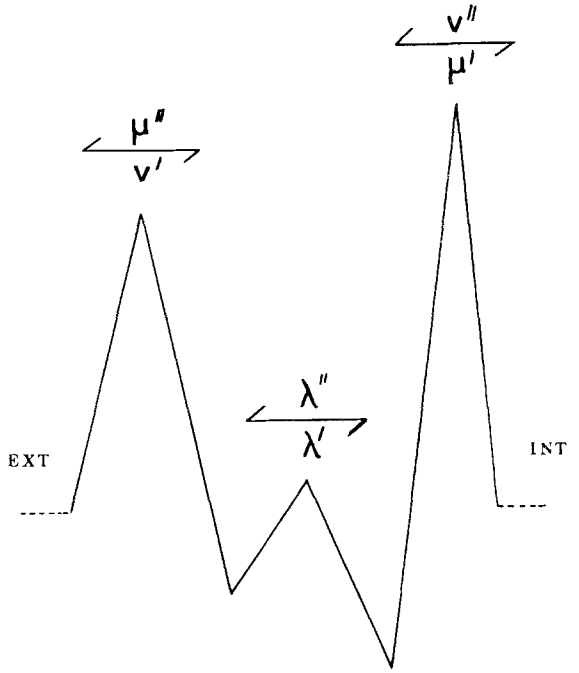

Fig. 6. Two-site, three-barrier model for permeation of monovalent cations through the ATP channel. It is assumed that the barriers and sites for monovalent cations are evenly spaced and that the barrier in the middle is low. For Mg^{2+}, only one site is postulated, accessible from the internal solution, but separated from the external one by an infinitely high barrier

All the data with monovalent cations have been fitted using special cases of Eq. (A3)

Experiments with excised patches show that Na^+ blocks the current from the inside, but not from the outside. From the denominator of Eq. (A3) and recalling the definition of Q in Eq. (A2), with i = Na, one sees that this finding suggests

$$\bar{\nu}'_{Na} \ll \bar{\nu}''_{Na} \tag{A4}$$

and consequently $M_{Na} \simeq 1$ [*see* definition of M_{Na} in Eq. (A2)]. As a consequence of condition (A4), and from considerations on Eqs. (A3) and (A2), it can be shown that the term proportional to the activity of external Na^+, a'_{Na}, in the denominator of Eq. (A3) can be neglected altogether. Thus, when sodium is present only outside, Eq. (A3) reduces to

$$I = -F \frac{\nu'_K(a'_K e^{-\phi/2} - a''_K e^{\phi/2}) + M_K \bar{\nu}'_{Na} a'_{Na} e^{-\phi/2}}{M_K e^{-\phi/3} + Q_K}. \tag{A5}$$

Equation (A5) has been used to fit the data in Fig. 2. It contains five independent parameters: for example, $\bar{\nu}'_K$, $\bar{\nu}''_K$, $\bar{\mu}'_K$, $\bar{\mu}''_K$, and $\bar{\nu}'_{Na}$.

In the experiments of Fig. 3, where Na^+ was present only inside, K^+ was 140 mM on both sides. Considering that $\bar{\nu}'_{Na} \ll \bar{\nu}'_K$, the term proportional to the sodium activity in the numerator of Eq. (A3) is sufficiently small that it can be neglected. After slight rearrangements in the denominator, one finds

$$I = F \frac{2\bar{\nu}'_K a_K \sinh \frac{\phi}{2}}{M_K e^{-\phi/3} + Q_K + M_K[(e^{\phi/3}/\bar{K}^{c}_{Na}) + 1/\bar{K}^{i}_{Na}]a''_{Na}}. \tag{A6}$$

Equation (1) in the Results section is the reciprocal of the ratio of Eq. (A6) to the corresponding one for zero Na^+ activity.

B) Blocking by Mg^{2+}

Postulating the presence of a single blocking site for magnesium in the channel located at an "electrical distance," α, from the internal solution, the current, in symmetrical K^+ and with Mg^{2+} present only inside, is

$$I = F \frac{2\bar{\nu}'_K a_K \sinh \frac{\phi}{2}}{M_K e^{-\phi/3} + Q_K + M_K e^{2\alpha\phi} C''_{Mg}/\bar{K}_{Mg}}. \tag{A7}$$

Equation (2) in the Results section is the reciprocal of the ratio of Eq. (A7) to the corresponding one for zero magnesium.